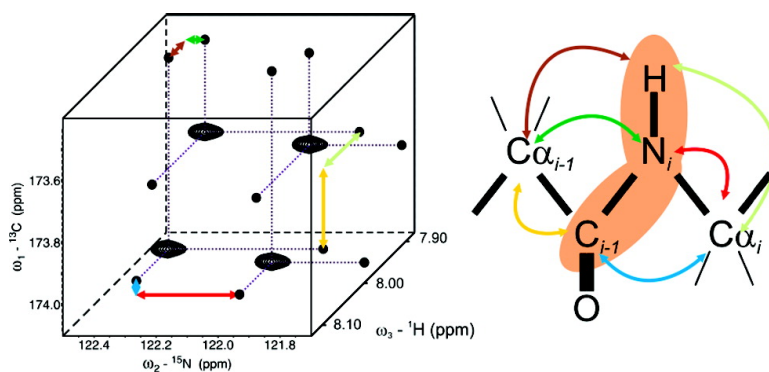## Communication

Determination of Spin#Spin Couplings from Ultrahigh Resolution 3D NMR Spectra Obtained by Optimized Random Sampling and Multidimensional Fourier Transformation

Krzysztof Kazimierczuk, Anna Zawadzka, Wiktor Koz#min#ski, and Igor Zhukov

More About This Article

Additional resources and features associated with this article are available within the HTML version:

- Supporting Information
- Access to high resolution figures
- Links to articles and content related to this article
- Copyright permission to reproduce figures and/or text from this article

View the Full Text HTML

Determination of Spin−Spin Couplings from Ultrahigh Resolution 3D NMR Spectra Obtained by Optimized Random Sampling and Multidimensional Fourier Transformation

Krzysztof Kazimierczuk,[†] Anna Zawadzka,[†] Wiktor Koźmiński,*,[†] and Igor Zhukov*,[‡,§]

Department of Chemistry, University of Warsaw, Pasteura 1, 02-093 Warsaw, Poland, Slovenian NMR Centre, National Institute of Chemistry, Hajdrihova 19, SI-1001 Ljubljana, Slovenia, and Institute of Biochemistry and Biophysics, Polish Academy of Sciences, Pawińskiego 5a, 02-106 Warsaw, Poland

Received January 25, 2008; E-mail: kozmin@chem.uw.edu.pl; igor.zhukov@ki.si

Backbone scalar couplings (J) are widely used in NMR studies of biomolecular structure and dynamics.[1] For many years, the vicinal ^3J scalar couplings were mostly used for the evaluation of φ and ψ backbone torsion angles in proteins with the aid of the Karplus relationship.[2] Several ^3J couplings have been parametrized with respect to φ and ψ angles for different proteins.[3,4] Presently, there is considerable interest in precise determination of one-bond and two-bond couplings for structural studies of weakly oriented biomolecules.[5] The one-bond $^1J_{N(i)C\alpha(i)}$ and two-bond $^2J_{N(i)C\alpha(i-1)}$ couplings were determined from the J-modulated HSQC experiment,[6,7] 3D HNCO experiment using spin-state selections,[8] or by a modification of IPAP HSQC experiment.[9] The combination of ZQ/DQ spectra was also used to obtain different carbon−carbon or carbon−nitrogen coupling constants[10] through one or two bonds.

Usually, the two-bond and three-bond backbone J coupling constants span the range of a few hertz. To measure these values, it is necessary to use long maximum evolution times because peak line width decreases with increasing acquisition time. The natural minimum width of the signal is determined by relaxation processes. In conventional multidimensional NMR experiments, this minimum peak line width can hardly be reached because of the respective sampling restrictions. The Nyquist theorem limits the maximum phase accumulated between subsequent data points to π radians. Thus, the width of the correctly transformed frequency band is inversely proportional to the delay between consecutive evolution time points. Overestimation of this delay causes signal aliasing. Therefore, one must choose between good spectral resolution (narrow lines) and a wide spectral band due to the Nyquist theorem limitation combined with the reciprocal relation between the line width and the acquisition time. However, the use of nonlinear sampling allows one to overcome this limitation.

There are several approaches to nonconventional NMR signal sampling and processing of the respective data sets.[11–20] Recently, we have shown that multidimensional Fourier transformation (MFT) of a randomly sampled NMR signal yields properly scaled and well-resolved spectra at sampling density level equal to a few percent of that for conventional sampling.[21–23] We have also demonstrated that MFT, similarly to the conventional approach, requires neither a priori knowledge of spectrum nor additional parameters. MFT was also successfully applied to nonconventionally sampled NMR data sets by other groups.[24–26]

Random sampling of evolution time space does not cause signal aliasing as there is no constant delay between consecutive time

† University of Warsaw.
‡ National Institute of Chemistry.
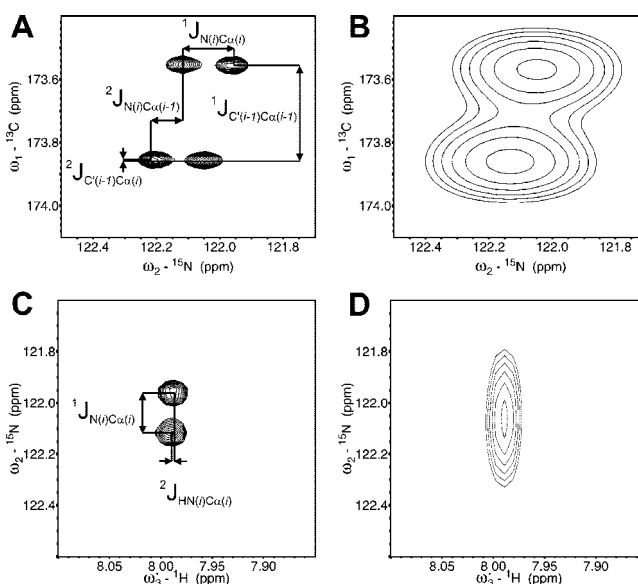§ Polish Academy of Sciences.

Figure 1. Comparison of spectral planes obtained for K48 signal in Cα-coupled 3D HNCO spectrum of 1.5 mM human ubiquitin solution. Panels A,B and C,D show F_1F_2 and F_2F_3 spectrum cross-sections, respectively. The spectra were obtained by optimized random sampling (A,C) with Gaussian distribution using σ of 62.5 and 100 ms for t_1 and t_2, respectively, and by conventional sampling (B,D), using 4900 evolution time points in both cases. For the random sampling, maximum evolution times for t_1 and t_2 were 125 and 200 ms, respectively. In the conventional experiment, the spectrum was acquired using a 70×70 sampling grid. In both cases, spectral widths of 3000, 2300, and 12 000 Hz were set in F_1, F_2, and F_3 dimensions, respectively. The spectra were processed using $2048 \times 1024 \times 2048$ real points. The conventional time domain data were apodized using cosine square function for all dimensions, while for the MFT, apodization was applied in the F_3 dimension only. The experiments were acquired on 700 MHz Varian NMR Systems spectrometer at 298 K.

domain points.[22] Instead of the aliasing, one obtains an artifactual "sampling noise". However, this approach yields ultrahigh resolution at a level of artifacts[22,23] which is tens times lower than peak amplitude, even at a few percent of Nyquist density.

When using conventional data acquisition, the resolution requirements necessary for measuring coupling constants are fulfilled in most 2D NMR spectra. However, 2D NMR techniques work relatively well only for small (molecular mass <10 kDa) folded proteins featuring well-resolved chemical shifts.

In this work, we have used the MFT method to obtain a 3D Cα-coupled HNCO spectrum. Ultrahigh resolution in indirectly detected dimensions enabled us to determine a number of backbone J coupling values. In a 30 h experiment, t_1/t_2 domain was sampled
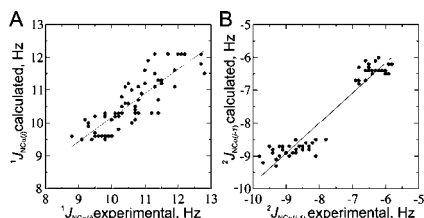
Figure 2. Plots of calculated versus experimental values of $^1J_{N(i)C\alpha(i)}$ (A) and $^2J_{N(i)C\alpha(i-1)}$ (B) coupling constants for human ubiquitin. The coupling constants were parametrized using the torsion angles from Protein Data Bank,[32] as follows: (A) $^1J_{N(i)C\alpha(i)} = 10.176 - 0.987 \cdot \cos[\psi(i)] + 1.080 \cdot \cos[2 \cdot \psi(i)]$, linear correlation coefficient $R = 0.854$; and (B) $^2J_{N(i)C\alpha(i-1)} = -7.21 + 1.41 \cdot \cos[\psi(i-1) + 33] - 0.42 \cdot \cos[2 \cdot (\psi(i-1) + 33)] - 0.47 \cdot \cos[\varphi(i-1)]$, $R = 0.962$. Comparison of analogous plots using relationships obtained in previous studies is provided in the Supporting Information.

using 4900 points of optimized random sampling schedule.[23] The maximum evolution times were long enough to obtain almost natural line widths, whereas the sampling density reached 2.85% of that necessary for evenly spaced sampling. A conventional experiment of the same resolution would have required almost 49 days. The standard 3D HNCO pulse sequence with semiconstant time evolution of ^{15}N for t_2[27] was modified by removing all Cα inversion pulses during ^{13}C and ^{15}N evolution periods. Due to the optimized sampling schedule, the artifact levels in the signals' vicinity were about 3% of respective signal amplitudes. Moreover, the artifacts can be removed by employing a previously described cleaning procedure.[23]

Examplary cross-sections showing the resonance of K48 are shown in Figure 1. Four out of six possible couplings involving passive Cα(i) and Cα(i−1) nuclei ($^1J_{N(i)C\alpha(i)}$, $^2J_{N(i)C\alpha(i-1)}$, $^1J_{C'(i-1)C\alpha(i-1)}$, and $^2J_{C'(i-1)C\alpha(i)}$) are marked in the F_1/F_2 cross-section given in panel A. Note that peaks slightly differ in F_3 frequency. The two additional couplings $^2J_{HN(i)C\alpha(i)}$ and $^3J_{HN(i)C\alpha(i-1)}$ involve H$_N$ protons; the first of these couplings (for the resonance of G47) is shown in the F_2/F_3 cross-section presented in panel C. All the coupling constants were determined by a 3D peak-picking procedure implemented in the Sparky software.[28] The information on relative signs of the coupling values was obtained taking into account the presence of 3D E.COSY multiplet[29] and negative γ ratio for ^{15}N nuclei.

Considering that measured line widths are between 7 and 15 Hz, the analyzed spectra show excellent resolution and enable reliable and accurate detection of backbone J coupling constants of 1 Hz or less. Taking into account the digital resolution used and signal-to-noise ratio achieved, the accuracy of J coupling constant measurements in this study can be estimated at ± 0.3 Hz. However, this estimate involves no correction for differential relaxation effects.[30,31]

The measurement of $^2J_{N(i)C\alpha(i-1)}$ is of special interest since this constant reflects the secondary structure of proteins.[9] Recently, 44 out of 72 existing $^2J_{N(i)C\alpha(i-1)}$ coupling constants for human ubiquitin were determined based on a 2D ZQ/DQ HNCO spectrum.[10] The remaining constants could not be determined due to signal overlap. The approach proposed in the present study allowed us to successfully evaluate all couplings, with the exception of couplings for E24 and G75 residues, which were inaccessible owing to fast backbone amide proton exchange. The relation between $^2J_{N(i)C\alpha(i-1)}$ coupling constants and ψ backbone torsion angles, which corresponds directly to the secondary protein structure, has already been reported.[6,7,9,10] The $^2J_{N(i)C\alpha(i-1)}$ coupling constants measured in this study are in good agreement with previously published values,[10] with a correlation coefficient of 0.987.

The parametrization of $^2J_{N(i)C\alpha(i-1)}$ couplings with respect to φ and ψ angles and the correlations between expected and experimentally determined coupling values are shown in Figure 2.

In conclusion, we have shown that simple 3D NMR experiments, with random sampling of the evolution time space and MFT processing, enable achieving ultrahigh resolution spectra. The Cα-coupled 3D HNCO spectrum obtained in this way allows precise measurement of six coupling constants involving passive Cα spin. The measured J coupling values provide information about backbone torsion angles at early stages of protein structure determination. The technique offered can be used for the determination of various residual dipolar couplings and for resolving chemical shifts in partially unfolded proteins.

Supporting Information Available: Table containing all the coupling constants determined for ^{13}C,^{15}N-labeled human ubiquitin in this study, and a graphical representation of calculated versus experimental coupling constants obtained based on Karplus relationships from previous studies. This material is available free of charge via the Internet at http://pubs.acs.org.

References
(1) Eberstadt, M.; Gemmecker, G.; Mierke, D. F.; Kessler, H. *Angew. Chem., Int. Ed. Engl.* **1995**, *34*, 1671–1695.
(2) Karplus, M. *J. Am. Chem. Soc.* **1963**, *85*, 2870–2871.
(3) Bax, A.; Vuister, W. G. *J. Am. Chem. Soc.* **1993**, *115*, 7772–7777.
(4) Wang, A. C.; Bax, A. *J. Am. Chem. Soc.* **1995**, *117*, 1810–1813.
(5) Tjandra, N.; Bax, A. *Science* **1997**, *278*, 1111–1114.
(6) Wirmer, J.; Schwalbe, H. *J. Biomol. NMR* **2002**, *23*, 47–55.
(7) Wienk, H. L. J.; Martinez, M. M.; Yalloway, G. N.; Schmidt, J. M.; Pérez, C.; Rüterjans, H.; Löhr, F. *J. Biomol. NMR* **2003**, *25*, 133–145.
(8) Permi, P.; Rosevear, P. R.; Annila, A. *J. Biomol. NMR* **2000**, *17*, 43–54.
(9) Ding, K.; Gronenborn, M. A. *J. Am. Chem. Soc.* **2004**, *126*, 6232–6233.
(10) Koźmiński, W.; Zhukov, I.; Pecul, M.; Sadlej, J. *J. Biomol. NMR* **2005**, *31*, 87–95.
(11) Kupče, Ē.; Freeman, R. *J. Am. Chem. Soc.* **2003**, *125*, 13958–13959.
(12) Kupče, Ē.; Freeman, R. *Concepts Magn. Reson.* **2004**, *22A*, 4–11.
(13) Malmodin, D.; Billeter, M. *J. Am. Chem. Soc.* **2005**, *127*, 13486–13487.
(14) Orekhov, V.; Ibraghimov, I.; Billeter, M. *J. Biomol. NMR* **2003**, *27*, 165–173.
(15) Tugarinov, V.; Kay, L. E.; Ibraghimov, I.; Orekhov, V. Y. *J. Am. Chem. Soc.* **2005**, *127*, 2767–2775.
(16) Mandelshtam, V. A.; Taylor, H. S.; Shaka, A. J. *J. Magn. Reson.* **1998**, *133*, 304–312.
(17) Rovnyak, D.; Frueh, D. P.; Sastry, M.; Sun, Z.-Y. J.; Stern, A. S.; Hoch, J. C.; Wagner, G. *J. Magn. Reson.* **2004**, *170*, 15–21.
(18) Snyder, D. A.; Xu, Y.; Yang, D.; Brüschweiler, R. *J. Am. Chem. Soc.* **2007**, *129*, 14126–14127.
(19) Frydman, L.; Scherf, T.; Lupulescu, A. *Proc. Natl. Acad. Sci. U.S.A.* **2002**, *99*, 15858–15662.
(20) Schanda, P.; Kupče, Ē.; Brutscher, B. *J. Biomol. NMR* **2005**, *33*, 199–211.
(21) Kazimierczuk, K.; Koźmiński, W.; Zhukov, I. *J. Magn. Reson.* **2006**, *179*, 323–328.
(22) Kazimierczuk, K.; Zawadzka, A.; Koźmiński, W.; Zhukov, I. *J. Biomol. NMR* **2006**, *36*, 157–168.
(23) Kazimierczuk, K.; Zawadzka, A.; Koźmiński, W.; Zhukov, I. *J. Magn. Reson.* **2007**, *188*, 344–356.
(24) Coggins, B. E.; Zhou, P. *J. Magn. Reson.* **2007**, *184*, 207–221.
(25) Pannetier, N.; Houben, K.; Blanchard, L.; Marion, D. *J. Magn. Reson.* **2007**, *186*, 142–149.
(26) Gledhill, J. M.; Wand, A. J. *J. Magn. Reson.* **2007**, *187*, 363–370.
(27) Sattler, M.; Schleucher, J.; Griesinger, C. *Prog. NMR Spectrosc.* **1999**, *34*, 93–158.
(28) Goddard, T. D.; Kneller, D. G. *SPARKY 3*; University of California, San Francisco.
(29) Griesinger, C.; Sorensen, O. W.; Ernst, R. R. *J. Am. Chem. Soc.* **1985**, *107*, 6394–6396.
(30) Harbison, G. S. *J. Am. Chem. Soc.* **1993**, *115*, 3026–3027.
(31) Rexroth, A.; Schmidt, P.; Szalma, S.; Geppert, T.; Schwalbe, H.; Griesinger, C. *J. Am. Chem. Soc.* **1995**, *117*, 10389–10390.
(32) Cornilescu, G.; Marquardt, J. L.; Ottiger, M.; Bax, A. *J. Am. Chem. Soc.* **1998**, *120*, 6836–6837.; PDB ID: 1D3Z.

JA800622P